Radium isotopes to investigate the water mass pathways on the Kerguelen Plateau (Southern Ocean)

van Beek P.[1,*], Bourquin M.[1], Reyss J-L. [2], Souhaut M. [1], Charette M.A.[3] and Jeandel C. [1].

[1]LEGOS, Laboratoire d'Etudes en Géophysique et Océanographie Spatiales (CNRS/CNES/IRD/UPS), Observatoire Midi Pyrénées, 14 avenue Edouard Belin, 31400 Toulouse, France
[2] LSCE (CNRS/CEA/UVSQ), Laboratoire des Sciences du Climat et de l'Environnement, avenue de la Terrasse, 91198 Gif-sur-Yvette, France
[3] Department of Marine Chemistry and Geochemistry, Woods Hole Oceanographic Institution, 266 Woods Hole Road, Woods Hole, MA 02543, USA

* Corresponding author
Tel. + 33 (0)5 61 33 30 51
Fax + 33 (0)5 61 25 32 05
Email : vanbeek@legos.obs-mip.fr

Abstract

Natural iron fertilization promotes the phytoplankton bloom that takes place on the Kerguelen Plateau in the Indian sector of the Southern Ocean. We measured ^{228}Ra ($T_{1/2}$=5.75 y) and ^{226}Ra ($T_{1/2}$=1602 y) in waters above the Kerguelen Plateau in order to provide information on the water mass pathways, which in turn could help elucidate the mechanisms controlling iron fertilization in that area. ^{228}Ra activities are extremely low in this region, being in most cases <0.15 dpm/ 100 kg (< $2.5.10^{-18}$ g kg^{-1}). Station A3 (520 m depth), located on the plateau in the middle of the bloom area, also displays such low values but with higher ^{228}Ra activities (and higher ^{228}Ra/^{226}Ra ratios) in the upper 150 m. Such a pattern suggests the presence of a water mass that recently interacted with sediments and therefore has been advected onto the Kerguelen Plateau. Elevated ^{228}Ra activities were found in shallow waters in the vicinity of Heard Island, south of the Kerguelen Plateau. Contact of the water masses with the shallow lithogenic sediments present in that area likely explains these high ^{228}Ra activities. When combined with physical observations, these results suggest that the water mass advected onto the plateau originates from the south of the Kerguelen Plateau. This

northward advection might represent a supply of dissolved and/or particulate Fe for the observed phytoplankton bloom.

Using the ^{228}Ra profile obtained at station A3, we could estimate the vertical eddy diffusivity (K_z) on the Kerguelen Plateau. Our K_z estimate ($1.5.10^{-4} \pm 1.3.10^{-4}$ m^2 s^{-1}) compares well with that reported by Park et al.(this issue-a) based on CTD/ LADCP data. By combining this K_z estimate with the gradient of dissolved Fe observed at A3 (Blain et al., this issue), we calculate a vertical Fe flux of 1.0-14.3 nmol m^{-2} d^{-1}.

Keywords : radium, vertical eddy diffusivity, ocean circulation, Southern Ocean, iron

1. Introduction

^{226}Ra ($T_{1/2}$ = 1602 years) and ^{228}Ra ($T_{1/2}$ = 5.75 years) have been widely used as tracers of water masses and to provide rates of mixing in the ocean (Koczy, 1958; Moore, 1972; Li et al., 1980; Sarmiento et al., 1982; Moore et al., 1986; Rutgers van der Loeff et al., 1995). The global oceanic distribution of ^{226}Ra and ^{228}Ra was well-documented during the GEOSECS and TTO programs (Broecker et al., 1967; Li et al., 1973; Kaufman et al., 1973; Broecker et al., 1976; Ku and Lin, 1976; Chan et al., 1976; Ku et al., 1980).

^{226}Ra and ^{228}Ra are supplied to the ocean by diffusion from deep-sea and continental shelf sediments after being produced in the sediments by ^{230}Th and ^{232}Th, respectively. With its half-life of 5.75 y, ^{228}Ra is particularly adapted to investigate mesoscale oceanographic processes. Highest activities are reported in coastal seas where waters are enriched in ^{228}Ra due to diffusive input from the sediments (Moore, 1969), riverine input (Moore et al., 1986) or submarine groundwater discharge (e.g. Moore, 1996). The ^{228}Ra activity of these water masses then decreases with increasing distance from the source, as a result of dilution (mixing) and radioactive decay. ^{228}Ra could thus be used to trace water masses that entered in

contact with the shelf or deep-sea sediments (Rutgers van der Loeff, 1994; Rutgers van der Loeff et al., 1995) but also to estimate horizontal mixing rates between the shelf and the open ocean (Moore, 2000).

In the open ocean, ^{228}Ra activities are usually highest in the upper water column - typically ca. 1-3 dpm/ 100 kg (17-50 ag kg^{-1}; *a* for *atto,* 10^{-18}) in the Atlantic Ocean and an order of magnitude lower in the Pacific ocean (Moore, 1969; Kaufman et al., 1973; Li et al., 1980; van Beek et al., 2007) - and decrease rapidly through the permanent pycnocline (Kaufman et al., 1973; Li et al., 1980; Moore, 1987). ^{228}Ra activities increase again close to the bottom. The high ^{228}Ra activities in the upper water column and in bottom waters reflect lateral transport of ^{228}Ra that diffused from shelf sediments and release from deep-sea sediments, respectively. The low activities in intermediate waters reflect the slow vertical mixing compared to radioactive decay. From the vertical distribution of ^{228}Ra, vertical mixing rates could thus be estimated, both in the deep-sea bottom boundary layer (Sarmiento et al., 1976; Sarmiento et al., 1982) and in the thermocline (Moore, 1972; Li et al., 1980; Ku et al., 1995).

^{228}Ra data are scarce in the Southern Ocean. Kaufman et al. (1973) and Li et al. (1980) reported activities for several surface samples. Most values were found to be close to detection limits (< 0.1 dpm/ 100 kg or < 1.7 ag kg^{-1}), while higher ^{228}Ra activities were found close to the Antarctic continent (0.5 dpm/ 100 kg; Kaufman et al., 1973). The Atlantic sector is the region of the Southern Ocean that has been most investigated for ^{228}Ra, with the first extensive work - including samples collected at depth - conducted during a transect across the Antarctic Circumpolar Current (Rutgers van der Loeff, 1994). Hanfland (2002) further contributed to increase the ^{228}Ra dataset in that sector. The Indian sector of the Southern Ocean has been poorly investigated, with only few surface values reported by Kaufman (1973) and few deep ^{228}Ra activities reported by Moore and Santschi (1986).

High biological productivity takes place on the Kerguelen Plateau in the Indian sector of the Southern Ocean although it is known to be a High Nutrient-Low Chlorophyll (HNLC) region (Blain et al., 2001; Blain et al., 2007). Natural iron fertilization derived from sediments on the plateau is suspected as the driver for this productivity anomaly. We proposed to measure the distribution of ^{228}Ra and ^{226}Ra on the Kerguelen Plateau in order to provide information on the water mass pathways, which could help elucidate the mechanisms controlling iron fertilization in that area.

2. MATERIAL AND METHODS

2.1 Stations investigated during the KEOPS project (A3, B1, B5, C1, C5, C11, Kerfix)

The KEOPS campaign took place between 19 January and 13 February 2005 on board the RV Marion Dufresne (Institut Polaire Français Paul Emile Victor/ Terres Australes et Antarctiques Françaises). Three transects (A, B, C) were conducted on and off the Kerguelen Plateau (that is, inside and outside the phytoplankton bloom; Fig. 1). A comparison of contrasting conditions (bloom region versus HNLC) allows us to provide information on the mechanisms of natural iron fertilization that takes place on the Kerguelen Plateau (Blain et al., 2007; Blain et al., this issue).

Among the 34 stations visited during KEOPS, six stations were selected for conducting the radium analyses. Two deep stations located east and west of the Kerguelen Plateau were investigated and can be considered as HNLC-type stations (Fig. 1; Table 1). First, Kerfix station is located west of the Kerguelen Plateau and southwest of the Kerguelen Islands (50° 40'S, 68° 25'E; 1650 m depth). Station Kerfix (for “Kerguelen Fixed station”) used to be a time-series station between 1990 and 1995 where hydrological and biological variables were measured once a month (Jeandel et al., 1998). Second, C11 (3435 m depth) is

located east of the Kerguelen Plateau. Seawater was collected for radium analyses at Kerfix on 11-12 February 2005, while station C11 was sampled on 25-28 January 2005.

Five stations located on the Kerguelen Plateau were also investigated (Fig. 1; Table 1). Based on real-time MODIS-MERIS composite images, station A3 (520 depth) was identified as a station located in the middle of the bloom area and was thus visited 5 times during KEOPS. A3 was sampled three times for radium (A3-3, 23-24 January 2005; A3-4, 03-04 February 2005; A3-5, 11-13 February 2005). Station B5 (530 m depth) was also sampled in the bloom area (31 January-1 February 2005) while B1 (384 m depth) was sampled outside the bloom (2 February 2005), being located on the western flank of the plateau. Finally, two stations - also located outside the bloom - were investigated on the southern flank of the plateau: station C1 (150 m depth; 8-9 February 2005) and station C5 (566 m; 7-8 February 2005). Note that station C1 was a very shallow station (150 m depth) located in the vicinity of Heard Island, south of the Kerguelen Plateau.

2.2 Collection of seawater samples and separation of radium isotopes

2.2.1 Sample collection

The collection of large volumes of seawater is required to analyze the very low ^{228}Ra activities characterizing waters from the Southern Ocean. During KEOPS, several techniques aimed at separating Ra isotopes from large volumes of seawater were used (Bourquin et al., submitted). Large volumes of seawater were collected using either: i) the "OISO" seawater supply used for the continuous pCO_2 analysis (as part of the OISO program, Océan Indien Service d'Observations) and/ or the ship's seawater intake that supplies the wet laboratory; ii) an *in situ* pump that returns water to the deck via a hose with a flow rate of 50 l min^{-1}, allowing us to collect samples from up to 120 m (Trull and Armand, 2001); or iii) 12-liter Niskin bottles, allowing the collection of samples from full ocean depth. For the latter

case, up to 12 Niskin bottles were fired for a single depth in order to provide ca. 140 kg seawater for one sample. For this method, vertical profiles of ^{228}Ra at a given station were obtained from a series of successive CTD casts. Techniques aimed at extracting radium isotopes *in situ* have also been tested (see below).

2.2.2 Radium extraction

We used MnO_2-coated acrylic fibres - so called, "Mn-fiber" - to extract radium isotopes from the seawater samples (Moore and Reid, 1973; Moore, 1976; Moore et al., 1985; Charette et al., 2001; van Beek et al., 2007; Charette et al., submitted). Seawater collected using either the "OISO" seawater supply (referred to as "OISO" in Table 1), *in situ* pump that returns water to the deck via a hose (referred to as "Pump" in Table 1) or Niskin bottles (referred to as the number of the associated CTD cast in Table 1) was passed by gravity on a PVC column filled with Mn-fiber at low flow rate (< 200 ml min^{-1}), providing an extraction efficiency of 100 % for Ra. Once on station, a column filled with Mn-fiber was also attached directly to the ship's seawater supply and forced through the fiber at a flow rate < 1 l min^{-1} followed by a flowmeter to record the volume of seawater that was filtered. These latter samples are referred to as "UW" in Table 1. In particular, the long stay at station C11 allowed us to filter up to ~3,000 litres through Mn-fiber.

Once back in the laboratory, the Mn-fibers were ashed (16 hours at 820°C) and transferred into sealed vials for gamma counting (Charette et al., 2001; van Beek et al., 2007).

2.2.3 *In situ* extraction of radium

During KEOPS, *in situ* pumps (Challenger Oceanic and MacLane pumps) were deployed in order to filter large volumes of seawater to collect suspended particles. Cartridges impregnated with MnO_2 (e.g. Hytrex-brand) placed in series after the filter have often been

used by geochemists to separate radionuclides - including radium - from seawater (Bacon and Anderson, 1982; Rutgers van der Loeff and Berger, 1993; Baskaran et al. 1993; Rutgers van der Loeff, 1994; Hanfland, 2002; Geibert et al., 2002). Rather than using cartridges impregnated with MnO_2, we filled the space in the middle of an untreated Hytrex cartridge with MnO_2 fiber. Doing so, we prevent the lengthy chemical treatment required for the separation of Ra isotopes when using impregnated cartridges. As is the case for cartridges impregnated with MnO_2, we placed fiber-packed Hytrex cartridges in series. Yield of radium fixation was determined by comparison with the ^{226}Ra activity of a sample collected at the same depth with Niskin bottles and filtered by gravity on Mn-fiber (Bourquin et al., submitted).

During the 4-h pump deployment at stations Kerfix and C11, we also suspended nylon nets filled with Mn-fibers to the frame of the *in situ* pumps so that large volumes of seawater could passively interact with the fiber (Kim et al., 2003; Charette et al., submitted). These samples are referred to as "Nylon" in Table 1. Because the volume of seawater that passed through the Mn-fiber is unknown, the ^{228}Ra activities in these samples are obtained by combining the $^{228}Ra/^{226}Ra$ ratio measured in these samples with the ^{226}Ra activity of a sample collected with Niskin bottles at the same depth.

2.3 Analytical Methods

Radium isotopes adsorbed on MnO_2 ash were counted at the underground laboratory of Modane (Laboratoire Souterrain de Modane, French Alps). High-efficiency, low-background, well-type germanium detectors (430 cm^3 and 950 cm^3) were used (Reyss et al., 1995). These detectors are shielded from cosmic radiation by 1700 m of rocks, which results in a very low background that allows for the measurement of very low activities. ^{226}Ra activities were determined using the ^{214}Pb (295 keV and 352 keV) and ^{214}Bi (609 keV) peaks.

^{228}Ra activities were determined using the 338 keV, 911 keV and 969 keV peaks of ^{228}Ac. Counting time for each sample ranged from 3 hours to 5 days (Table 1). Uncertainties reported for ^{226}Ra and ^{228}Ra activities are errors due to counting statistics (one standard deviation).

3. RESULTS

3.1 Hydrography

The general circulation in the region has been previously described by Park and Gamberoni (1995), Park et al.(1998a), Charrassin et al.(2004), but it is only during the KEOPS program that a detailed view of the circulation on and around the Kerguelen Plateau was obtained (Park et al., this issue-b). Hydrographic characteristics over the Kerguelen Plateau are discussed in details by Park et al.(this issue-b). A striking feature in this area is the presence of a water mass characterized by a subsurface temperature minimum centred at around 200 m called Winter Water (WW; Figs. 2, 3, 4). The WW was found at the stations investigated on and off the plateau, displaying variable temperature (Park et al., this issue-b). The Circumpolar Deep Water (CDW) lies just below the WW and can be decomposed into the i) Upper Circumpolar Deep Water (UCDW), which could be found on the plateau and ii) the Lower Circumpolar Deep Water (LCDW), which could be found at depths greater than 1400 m. Antarctic Bottom Water (AABW) is present below 2600 m (i.e. at station C11).

3.2 ^{226}Ra activities

The measurement of dissolved ^{226}Ra activities by gamma spectrometry typically requires ca. 10 kg of seawater. Because large volumes of seawater were collected for the ^{228}Ra analysis (> 100 kg), counting rates were high and uncertainties were low for ^{226}Ra (Table 1). ^{226}Ra activities on the plateau range from 13.7 dpm/ 100 kg (surface) to 17.5 dpm/ 100 kg

(near bottom). Note that repeated visits at station A3 show significant variability in the upper 200 m, while ^{226}Ra activities below this depth are relatively uniform. The deep open-ocean stations Kerfix and C11 exhibit comparable ^{226}Ra activities that range from 14.5 dpm/ 100 kg (surface) to 22.2 dpm/ 100 kg at 3300 m (station C11); Kerfix, however, had lower ^{226}Ra activities in the Winter Water (200 m depth) compared with station C11 (150 m depth).

3.3 ^{228}Ra activities and ^{228}Ra/^{226}Ra ratios

^{228}Ra activities are extremely low outside the plateau and also generally on the plateau. The detection of these very low activities was made possible because we used the very low background facility available at the underground laboratory of Modane (LSM) and also because large volumes of seawater were collected during KEOPS. Counting rates for ^{228}Ra were very low (Table 1), with samples rarely exceeding 100 net counts even after 3 days analyses. Higher count rates were obtained in samples collected *in situ* (using eg. Mn-fiber in nylon nets) or using the ship's seawater supply. Note that several samples exhibit very low counting rates (< 50 total net counts). Despite their low counting statistics, we did not reject these data because these counts were obtained during long counting sessions (5 days) (Table 1).

3.3.1 Stations off plateau

The ^{228}Ra activities at station Kerfix are < 0.15 dpm/ 100 kg throughout the water column with significantly higher values in the Winter Water and close to the bottom (Fig. 2). Station C11 shows a similar profile, with low values in surface and intermediate waters and slightly higher values between 20 m and 300 m. The highest activities found at station C11 are close to the bottom. The ^{228}Ra/^{226}Ra ratio displays a trend similar to that of ^{228}Ra. Note that two independent measurements of the ^{228}Ra/^{226}Ra ratio are available at stations Kerfix

(500 m) and C11 (200 m), with one value derived from the Niskin bottle sampling and one from the nylon net sample (Table 1). The two values are in good agreement.

3.3.2 Stations on the plateau

At station A3, ^{228}Ra activities are low at the surface (6 m) and below ~150 m, with values very similar to open-ocean stations (Fig. 3). We observe a slight enrichment in ^{228}Ra activities and in the ^{228}Ra/^{226}Ra ratio in the upper 150 m, just above the Winter Water. This enrichment is more obvious at A3-3 and A3-5 and can reach up to 0.25 dpm/ 100 kg at 100 m (A3-5). Note that we do not find significantly higher ^{228}Ra activities and ^{228}Ra/^{226}Ra ratios close to the bottom as was the case for the open-ocean stations. Stations C5 and B1 also show low ^{228}Ra activities. In contrast, station C5 (20 m) displayed a higher ^{228}Ra activity (0.39 dpm/ 100 kg) and a higher ^{228}Ra/^{226}Ra ratio (Fig. 4). The shallow station (C1) off Heard Island exhibits high ^{228}Ra activities as well (and ^{228}Ra/^{226}Ra ratios). The constant values found throughout the 150 m of the water column (0.28-0.36 dpm/ 100 kg) can be related to mixing driven by strong winds present during the sampling at station C1 (see the potential temperature profile, Fig. 4). Station B5 also exhibits slight ^{228}Ra enrichments in samples collected at 20 m and at 350 m (0.16 and 0.25 dpm/ 100 kg, respectively). Note that for sample collected close to the bottom at station B1, we measured an unexpectedly low ^{226}Ra activity, suggesting either a low recovery on the Mn-fiber or an error in the estimate of the volume that passed through the fiber; therefore, for this sample we report only the ^{228}Ra/^{226}Ra ratio (Table 1).

4. DISCUSSION

4.1 ^{226}Ra activities

The ^{226}Ra values reported here compare well with values reported for the Southern Ocean (Ku and Lin, 1976; Broecker et al., 1976; Hanfland, 2002). In particular, ^{226}Ra activities of surface waters from the Southern Ocean are much higher than surface waters from the Atlantic and Pacific Oceans (Broecker et al., 1967; Chung, 1974; Ku and Lin, 1976; Broecker et al., 1976; Chan et al., 1976; Chung and Craig, 1980), a feature that can be related to the upwelling at high latitudes of deep waters being enriched in ^{226}Ra (Ku and Lin, 1976). The ^{226}Ra variability observed in the upper 200 m, when sampling repeatedly station A3 - together with the ^{226}Ra/Ba variability that was also observed - will be discussed in another paper on the impact of biological activity and/or changes in the water mass pathways at this location.

4.2 ^{228}Ra activities and ^{228}Ra/^{226}Ra ratios

The low ^{228}Ra activities (and ^{228}Ra/^{226}Ra ratios) found in open-ocean stations and many stations located on the plateau are very similar to those reported by previous studies in the Southern Ocean: Kaufman et al.(1973) who report three surface values of 0.1-0.2 dpm/ 100 kg in the Indian Sector of the Southern Ocean, west of Kerguelen Island; Li et al.(1980) who report activities below detection limit (ie. < 0.1 dpm/ 100 kg) in the upper 200 m of stations from the Atlantic sector of the Southern Ocean; Rutgers van der Loeff (1994) who report values < 0.23 dpm/ 100 kg in waters away from the ^{228}Ra sources (shelf and bottom); and Hanfland (2002) who report ^{228}Ra in open-ocean surface waters as low as 0.02-0.07 dpm/ 100 kg (off the Antarctic Peninsula). The ^{228}Ra activities (and ^{228}Ra/^{226}Ra ratios) found at station C1, in the upper 150 m at station A3 and in surface waters at station C5 (0.25-0.39 dpm/ 100 kg) are significantly higher than the activities found in open-ocean waters. Therefore, these high activities suggest that these water masses have been enriched in ^{228}Ra through contact with shallow sediments.

^{228}Ra activities at station A3 do not show a significant increase close to the bottom as would be expected from a deep sedimentary source [see eg. increase of ^{228}Ra activities and ^{228}Ra/^{226}Ra ratios in bottom waters from open-ocean stations Kerfix and C11 (Fig. 2) or from stations B1 and B5 on the plateau (Fig. 4)]. In contrast, iron concentrations do increase with depth at station A3, implying that the shallow sediments of the plateau could constitute a source for iron (Blain et al., 2007; Blain et al., this issue). Enrichment in ^{228}Ra of a water mass in contact with the sediment is function of i) the residence time of this water mass over the sediment and ii) the intensity of the ^{228}Ra flux that diffuses out of the sediment, which depends on the ^{232}Th concentration in the sediment. Accumulation rates as well as the intensity of bioturbation also impact the sediment-derived radium flux (Cochran, 1980). In particular, high accumulation rates are associated with low radium flux (Fig. 4 of Cochran, 1980). Sediments from station A3 located under the phytoplankton bloom consist mainly of siliceous ooze that results from the accumulation of diatoms (Armand et al., this issue). Consequently, the lithogenic fraction containing ^{232}Th is highly diluted in these sediments (ca. 0.2 dpm g^{-1}; data not shown). ^{210}Pb$_{ex}$ activities measured in sediments from station A3 further indicate deep penetration and therefore high accumulation rates under the bloom (Reyss and van Beek, unpublished data). Taken together, the relatively low ^{232}Th activities in the sediment located under the bloom associated with high accumulation rates might result in relatively low ^{228}Ra fluxes diffusing out of the sediment at station A3, thereby explaining the relatively low ^{228}Ra activities in bottom waters at station A3. On the other hand, high diapycnal diffusivity was observed on the Kerguelen Plateau during KEOPS (see section 4.2.1.1; Blain et al., 2007; Park et al., this issue-a). Enhanced vertical mixing at station A3 would vertically transport the ^{228}Ra activity that diffused from the sediment, thus lowering the ^{228}Ra activity close to the bottom.

All the other stations located on the plateau - except C5 - do exhibit increased ^{228}Ra activities and ^{228}Ra/^{226}Ra ratios close to the bottom. Again, presence or absence of ^{228}Ra enrichments near the bottom may be related to the intensity of the ^{228}Ra flux diffusing out of the sediment and to the residence time of deep waters near the sediment.

4.2.1 Origin of the ^{228}Ra enrichments in upper waters at station A3

4.2.1.1 Vertical mixing

Strong diapycnal diffusivity (K_z) estimated from vertical density profiles (Osborn, 1980) was found during KEOPS based on CTD/ LADCP data (Blain et al., 2007; Park et al., this issue-a). Park et al. (this issue-a) report a K_z value of ~ 3.10^{-4} m^2 s^{-1} beneath the base of the mixed layer at station A3. This value is an order of magnitude higher than the most recent estimate of K_z in the Antarctic Circumpolar Current ($1.1.10^{-5}$ m^2 s^{-1}; Law et al., 2003) and indicates enhancement of the vertical mixing on the Kerguelen Plateau. This enhancement of vertical mixing, especially obvious when comparing time-series profiles of physical parameters (eg. potential temperature; Figs. 2, 3, 4), is likely due to internal wave activity.

Enhanced vertical mixing on the plateau is also expected to impact the distribution of ^{228}Ra, which, like Fe, diffuses out of the sediments. However, in contrast to the dissolved Fe profiles (Blain et al., 2007; Blain et al., this issue), ^{228}Ra activities on the plateau do not show significant increase close to the bottom. As discussed above, sediments from station A3 may not be a strong source for ^{228}Ra, while they may be a significant source for Fe. Consequently, the higher ^{228}Ra activities found in the upper 150 m at station A3 are unlikely to be generated by vertical mixing of the (low) ^{228}Ra activities found in bottom waters.

4.2.1.2 Lateral transport

Upwelling on the plateau of deep waters enriched in ^{228}Ra could generate a ^{228}Ra signal in surface waters at station A3. No isopycnal surfaces, however, rise toward the surface above the plateau, which allow us to rule out this hypothesis (Table 1). Consequently, lateral transport of ^{228}Ra-enriched waters on the plateau might best explain this signal. This implies interaction of a water mass with shallow sediments (< 200 m) so that the ^{228}Ra enrichment can be transferred horizontally in the upper 150 m of station A3. Shallow sediments can be found on the continental shelves of Kerguelen Island and Heard Island, north and south of the Kerguelen Plateau, respectively (Fig. 5).

A strong current is clearly established south of Kerguelen Island and circulates to the north-east along the eastern continental shelf break (Park and Gamberoni, 1997; Park et al., 1998b; Charrassin et al., 2004; Blain et al., 2007; Park et al., this issue-b; Mongin et al., this issue; Fig. 5). This current - which can be clearly seen on MODIS-MERIS images (Blain et al., 2007) - isolates the island from the Kerguelen Plateau, south-east of the island, and likely prevents significant transfer of shallow waters from the continental shelf towards the south. In contrast, Charrassin et al.(2004), based on temperature data collected by penguin-borne loggers, report a northwestward flow of surface and subsurface waters on the Kerguelen Plateau. They also suggested that this flow was consistent with the tidal residual circulation resulting from a tidal current-bottom topography interaction. Additionally, the mean flow measured at station A3 during KEOPS was heading to the NW, in agreement with the pattern observed by Charrassin et al.(2004). Note that current speed was weak on the plateau (< 0.05 m s^{-1}; Park et al., this issue-b). Waters that flow northwestward above the plateau may therefore have interacted with the shallow lithogenic sediments from the continental shelf of Heard Island (Fig. 5).

Sediment cores collected at station C1 indicate that the sediment in that area consists mainly in coarse grains of basalt. Contact of the water masses with these shallow lithogenic

sediments would increase their ^{228}Ra activity, as it was observed at station C1 (Figure 4). Zhang et al.(this issue) and Venchiarutti et al.(submitted) also report high concentrations of dissolved rare earth elements and dissolved ^{232}Th respectively in waters off Heard Island, which are attributed to the dissolution of lithogenic material possibly weathered from Heard Island. Because surface waters at stations C5 and A3 are also enriched in ^{228}Ra, this suggests that the ^{228}Ra enrichment observed on the shelf of Heard Island might be transferred along the southern flank of the Kerguelen Plateau (towards station C5; Fig. 5) and northwestward above the plateau (towards station A3; Fig. 5). Similar conclusions were reached based on the distribution of dissolved rare earth elements above the plateau (Zhang et al., this issue). The former circulation pattern agrees with the counterclockwise current (in the southern hemisphere) that would result along the slope from the interaction between tidal current and bottom topography (Charrassin et al., 2004).

4.2.2 Estimate of vertical mixing coefficient on the plateau

^{228}Ra profiles can be used to estimate vertical mixing either in the thermocline or in bottom waters (Moore, 1972; Li et al., 1980; Sarmiento et al., 1982; Ku et al., 1995). It has been proposed that enhanced vertical mixing over the plateau brings Fe from bottom waters that are enriched in Fe to surface waters (Blain et al., 2007; Blain et al., this issue). In contrast, ^{228}Ra activities over the plateau (A3) are higher in the upper water column as a result of lateral transport and decrease with depth. The vertical ^{228}Ra gradient (observed below the upper waters enriched in ^{228}Ra) can be used to calculate a vertical eddy diffusion coefficient.

A steady state is established when the supply of ^{228}Ra by mixing balances radioactive decay. If the mixing is vertical, the concentration as a function of depth is given by:

$$C_1=C_2 \exp\left(-[\lambda_{228}/K_z]^{1/2} z\right) \quad (1)$$

where C_1 and C_2 are concentrations at two depths; z is the depth interval; λ_{228} is the decay constant of ^{228}Ra; and K_z is the coefficient of vertical eddy diffusion. This simple model assumes that dispersion of ^{228}Ra could be approximated as a 1-D diffusive process (ie. no advection on the depth interval we consider) (Fig. 6). K_z can thus be calculated from the slope (m) of a plot of ln (^{228}Ra) versus water depth ($K_z=\lambda_{228}/ m^2$).

We calculated K_z at station A3-3 between 100 m and 400 m (ie. below the layer of waters enriched in ^{228}Ra). The activity at 450 m has been excluded from the calculation considering it likely reflects input from the sediment. On the plot ln (^{228}Ra) versus water depth, we obtain a slope (m) of 0.00511 ± 0.00229. The resulting K_z is $1.5.10^{-4} \pm 1.3.10^{-4}$ m^2 s^{-1}. This estimate should be considered cautiously, keeping in mind the steady-state assumption. However, the K_z that derives from the ^{228}Ra profile is in good agreement with the K_z estimated based on CTD/ LADCP data during KEOPS (Blain et al., 2007; Park et al., this issue-a). Between 180 m and 470 m, Park et al. (this issue-a) report a value of 0.8 ± 1.1 10^{-4} m^2 s^{-1}. As mentioned above, such a K_z is high (ie. higher than the most recent estimate of K_z for the Southern Ocean; Law et al., 2003) and suggests enhanced mixing over the plateau.

4.3 Implication for the understanding of the mechanisms controlling Fe fertilization on the Kerguelen Plateau

Combining our K_z estimate (100-400 m) with the vertical gradient of dissolved Fe observed at A3-3 for the same depths (0.059 nmol l^{-1} Fe at 100 m and 0.236 nmol l^{-1} Fe at 400 m; Blain et al., this issue), we obtain a potential vertical flux of Fe of 1.0-14.3 nmol m^{-2} d^{-1}. Blain et al.(2007) and Sarthou et al.(this issue) report a flux of dissolved Fe into surface waters of A3 significantly higher than our estimate (ie. 31 nmol m^{-2} d^{-1}) by combining the K_z deduced from CTD/ LADCP data between 100 m and 200 m and the vertical gradient of dissolved Fe observed on the same depth interval. Both estimates, however, are lower than the

net dissolved Fe requirements of phytoplankton (defined as the difference between uptake and regeneration rates of dissolved Fe; ie. 208 ± 77 nmol m^{-2} d^{-1}, Blain et al., 2007). This suggests an additional source of Fe. The atmospheric input of Fe (ie. transport of continental dusts originating from the Kerguelen Island) is considered to be insignificant above the Kerguelen Plateau (Wagener et al., submitted; Blain et al., this issue). Blain et al.(2007) calculated that, in addition to the vertical supply of Fe, either the ongoing depletion of the winter surface stock of Fe or dissolution of lithogenic particulate Fe could balance the demand. Because waters off Heard Island exhibit high dissolved Fe concentrations (0.5 nmol l^{-1}; Blain et al., this issue), it cannot be excluded also that the northward advection - as shown by the ^{228}Ra data and physical observations - supplies Fe to the Kerguelen Plateau. Such advection could contribute to the winter surface stock of Fe and/or to fertilize the phytoplankton bloom in that area.

We note, however, that chlorophyll *a* concentrations are relatively low in the southern part of the Kerguelen Plateau (ie. east/ north-east of Heard Island; Blain et al., 2007) and that dissolved Fe concentrations decrease rapidly away from Heard Island (Blain et al., this issue). Strong currents around Heard Island and on the southern slope of the Kerguelen Plateau (Park et al., this issue-b; Maraldi et al., in prep.) may prevent bloom formation in that area. The decrease of Fe away from Heard Island, which cannot be associated with the consumption by phytoplankton, raises the question of how far Fe originating from the shelf of Heard Island, south of the plateau, can be transported and how such lateral input can contribute to fertilize the bloom located on the northern part of the plateau. Based on the analysis of dissolved Rare Earth Element (REE) concentrations, Zhang et al. (this issue) calculated a potential Fe flux to the Kerguelen Plateau of from the Heard Island shelf of > 100 000 tons y^{-1}. Although most of this Fe is likely to be quickly removed from the water column (eg. via oxide/ hydroxide

precipitates), it cannot be excluded that a small fraction of this Fe contributes to the maintenance of the phytoplankton bloom.

5. Conclusion

The ^{228}Ra data suggest a northward advection over the Kerguelen Plateau of waters that have interacted with shallow lithogenic sediments from the continental shelf of Heard Island, south of the plateau. This pattern agrees with that deduced from the dissolved rare earth elements (Zhang et al., this issue) and with physical observations (Charrassin et al., 2004; Park et al., this issue-b). Because waters off Heard Island exhibit high dissolved Fe concentrations (Blain et al., this issue), the northward advection could also supply Fe to the Kerguelen Plateau. Although most of this Fe may be quickly removed from the water column by scavenging processes, this advection could either contribute to the winter surface stock of Fe and/or to initiate and sustain the annual phytoplankton bloom that takes place above the Kerguelen Plateau. In addition to the vertical supply of Fe and to the ongoing depletion of the winter surface stock of Fe, the Fe potentially transported by the northward advection - in dissolved and/or particulate forms - could partially balance the net dissolved Fe requirements of phytoplankton.

Acknowledgements – This work was supported by IPEV (Institut Paul Emile Victor) and INSU/ CNRS (Institut National des Sciences de l'Univers/ Centre National de la Recherche Scientifique). M.A.C. was supported by the National Science Foundation (ANT-0443869). We are grateful to the crew and captain of RV Marion Dufresne. We thank Stéphane Blain, PI of the KEOPS project and Bernard Quéguiner, chief scientist during KEOPS. We thank Aurélien Rojas at the underground laboratory of Modane (LSM) and Julian Thévenet who

started the gamma measurements during a master's project. We are grateful to the three anonymous reviewers; their comments improved significantly the quality of the paper.

References

Armand, L.K., Crosta, X., Quéguiner, B., Mosseri, J., Garcia, N. Diatoms in surface sediments of the Kerguelen-Heard region of the South Indian Ocean. Deep-Sea Research Part II, This issue.

Bacon, M.P., Anderson, R.F., 1982. Distribution of thorium isotopes between dissolved and particulate forms in the deep sea. Journal of Geophysical Research, 87, 2045-2056.

Baskaran, M., Murphy, D.J., Santschi, P.H., Orr, J.C., Schink, D.R., 1993. A method for rapid *in situ* extraction and laboratory determination of Th, Pb and Ra isotopes from large volumes of seawater, Deep-Sea Research Part I, 40, 849-865.

Blain, S., Sarthou, G., Laan, P. Distribution of dissolved iron during the natural iron fertilization experiment KEOPS (Kerguelen Island, Southern Ocean), Deep-Sea Research Part II, This issue.

Blain,S., Quéguiner, B., Armand, L., Belviso, S., Bombled, B., Bopp, L., Bowie, A., Brunet, C., Brussaard, C., Carlotti, F., Christaki, U., Corbière, A., Durand, I., Ebersbach, F., Fuda, J.-L., Garcia, N., Gerringa, L., Griffiths, B., Guigue, C., Guillerm, C., Jacquet, S., Jeandel, C., Laan, P., Lefèvre, D., Lo Monaco, C., Malits, A., Mosseri, J., Obernosterer, I., Park, Y.-H., Picheral, M., Pondaven, P., Remenyi, T., Sandroni, V., Sarthou, G., Savoye, N., Scouarnec, L., Souhaut, M., Thuiller, D., Timmermans, K., Trull, T., Uitz, J., van Beek, P., Veldhuis, M., Vincent, D., Viollier, E., Vong, L., Wagener, T., 2007. Effect of natural iron fertilization on carbon sequestration in the Southern Ocean, Nature, 446, 1070-1074.

Blain, S., Tréguer, P., Belviso, S., Bucciarelli, E., Denis, M., Desabre, S., Fiala, M., Martin Jezequel, V., Le Fevre, J., Mayzaud, P., 2001. A biogeochemical study of the island mass effect in the context of the iron hypothesis : Kerguelen Islands, Southern Ocean. Deep-Sea Research Part I, 48, 163-187.

Bourquin, M., van Beek, P., Reyss, J.-L., Souhaut, M., Charette, M., Testing methods to separate radium from large volumes of seawater, submitted to Marine Chemistry.

Broecker, W.S., Goddard, J., Sarmiento, J.L., 1976. The distribution of ^{226}Ra in the Atlantic Ocean. Earth and Planetary Science Letters, 32, 220-235.

Broecker, W.S., Li, Y.H., Cromwell, J., 1967. Radium-226 and Radon-222 : Concentration in Atlantic and Pacific Oceans. Science, 158, 1307-1310.

Chan, L.H., Edmond, J.M., Stallard, R.F., Broecker, W.S., Chung, Y.C., Weiss, R.F., Ku, T.L., 1976. Radium and barium at GEOSECS stations in the Atlantic and Pacific. Earth and Planetary Science Letters, 32, 258-267.

Charette, M.A., Gonnea, M.E., Morris, P., Statham, P., Fones, G., Planquette, H., Salter, I., Naveira Garabato, A., Radium as tracers of iron sources fueling a Southern Ocean phytoplankton bloom, submitted.

Charette, M.A., Buesseler, K.O., Andrews, J.E., 2001. Utility of radium isotopes for evaluating the input and transport of groundwater-derived nitrogen to a Cape Cod estuary, Limnology and Oceanography, 46 (2), 465-470.

Charrassin, J.B., Park, Y.-H., LeMaho, Y., Bost, C.-A., 2004. Fine resolution 3D temperature fields off Kerguelen from instrumented penguins, Deep-Sea Research Part I, 51, 2091-2103.

Chung, Y., Craig, H., 1980. ^{226}Ra in the Pacific Ocean. Earth and Planetary Science Letters, 49, 267-292.

Chung Y.-C., 1974. Radium-226 and Ra-Ba relationships in Antarctic and Pacific waters. Earth and Planetary Science Letters, 23, 125-135.

Cochran, J.K., 1980. The flux of Ra-226 from deep-sea sediments. Earth and Planetary Science Letters, 49, 381-392.

Geibert, W., Rutgers van der Loeff, M.M., Hanfland, C., Dauelsberg, H.-J., 2002. Actinium-227 as a deep-sea tracer : sources, distribution and applications. Earth and Planetary Science Letters, 198, 147-165.

Hanfland, C., 2002. Radium-226 and radium-228 in the Atlantic sector of the Southern Ocean, Berichte zur Polar und Meeresforschung 431, phD Thesis, Alfred Wegener Institute, Bremerhaven, Germany, 135pp.

Jeandel C., Ruiz-Pino, D., Gjata, E., Poisson, A., Brunet, C., Charriaud, E., Dehairs,F., Delille, D., Fiala, M., Fravalo, C., Miquel, J.C., Park,Y.-H., Pondaven, P., Quéguiner, B., Razouls, S., Shauer, B., Tréguer, P., 1998. KERFIX, a time-series station in the Southern Ocean : a presentation. Journal of Marine Systems, 17, 555-569.

Kaufman, A., Trier, R.M., Broecker, W.S., Feely, H.W., 1973. Distribution of ^{228}Ra in the world ocean. Journal of Geophysical Research, 78 (36), 8827-8848.

Kim, G., Hussein, N., Church, T., 2003. Tracing the advection of organic carbon into the subsurface Sargasso Sea using ^{228}Ra/^{226}Ra tracer. Geophysical Research Letters 30 (16), 1874, doi:10.1029/2003GL017565.

Koczy, F.F., 1958. Natural radium as a tracer in the ocean, Proc. 2nd U.N. Int. Conf. on peaceful uses of atomic energy 18, 351.

Ku, T.-L., Luo, S., Kusakabe, M., Bishop, J.K.B., 1995. ^{228}Ra-derived nutrient budgets in the upper equatorial Pacific and the role of "new" silicate in limiting productivity. Deep-Sea Research Part II, 42(2-3), 479-497.

Ku, T.-L., Huh, C.-A., Chen, P.S., 1980. Meridional distribution of ^{226}Ra in the eastern Pacific along GEOSECS cruise tracks. Earth and Planetary Science Letters, 49, 293-308.

Ku, T.-L., Lin, M.-C., 1976. ^{226}Ra distribution in the Antarctic Ocean. Earth and Planetary Science Letters, 32, 236-248.

Law, C., Abraham, E.R., Watson, A., Liddicoat, M., 2003. Vertical eddy diffusion and nutrient supply to the surface mixed layer of the Antarctic Circumpolar Current. Journal of Geophysical Research, 108, 3272.

Li, Y.-H., Feely, H. W., Toggweiler, J.R., 1980. ^{228}Ra and ^{228}Th concentrations in GEOSECS Atlantic surface waters, Deep-Sea Research. 27A, 545-555.

Li, Y.-H., Ku, T.L., Mathieu, G.G., Wolgemuth, K., 1973. Barium in the Antarctic Ocean and implications regarding the marine geochemistry of Ba and ^{226}Ra. Earth and Planetary Science Letters, 19, 352-358.

Maraldi, C., Testut, L., Coleman, R., Barotropic tides in the southern Indian Ocean, in preparation.

Mongin, M., Molina, E., Trull, T., Fade and shape of the Kerguelen Plateau phytoplankton bloom : a combined remote sensing and biogeochemical analysis of this natural iron fertilized environment. Deep-Sea Research Part II, This issue.

Moore, W.S., 2000. Determining coastal mixing rates using radium isotopes. Continental Shelf Research, 1993-2007.

Moore, W.S., DeMaster, D.J., Smoak, J.M., McKee, B.A., Swarzenski, P.W., 1996. Radionuclide tracers of sediment-water interactions on the Amazon shelf, Continental shelf Research, 16, 645-665.

Moore, W.S., 1987. Radium 228 in the South Atlantic Bight. Journal of Geophysical Research, 92, 5177-5190.

Moore, W.S., Sarmiento, J.L., Key, R.M., 1986. Tracing the Amazon Component of Surface Atlantic Water Using ^{228}Ra, Salinity and Silica, Journal of Geophysical Research. 91, 2574-2580.

Moore, W. S., Santschi, P.H., 1986. Ra-228 in the deep Indian Ocean, Deep-Sea Research. 33 (1), 107-120.

Moore, W.S., Key, R.M., Sarmiento, J.L., 1985. Techniques for precise mapping of ^{226}Ra and ^{228}Ra in the ocean. Journal of Geophysical Research, 90, 6983-6995.

Moore, W.S., 1976. Sampling ^{228}Ra in the deep ocean. Deep-Sea Research, 23, 647-651.

Moore, W.S., Reid, D.F., 1973. Extraction of radium from natural waters using manganese-impregnated acrylic fibers. Journal of Geophysical Research, 78, 8880-8886.

Moore W.S., 1972. Radium-228 : application to thermocline studies. Earth and Planetary Science Letters, 16, 421-422.

Moore, W.S., 1969. Oceanic Concentration of ^{228}Radium. Earth and Planetary Science Letters, 6, 437-446.

Osborn, T.R., 1980. Estimate of vertical diffusion from dissipation measurements. Journal of Physical Oceanography, 10, 83-89.

Park, Y.-H., Fuda, J.-L., Durand, I., Naveira Garabato, A.C., Internal tides and vertical mixing over the Kerguelen Plateau. Deep-Sea Research Part II, This issue-a.

Park, Y.-H., Roquet, F., Fuda, J.-L., Durand, I., Circulation over the Kerguelen Plateau. Deep-Sea Research Part II, This issue-b.

Park, Y.-H., Charriaud, E., Fieux, M., 1998a. Thermohaline structure of the Antarctic Surface Water/ Winter Water in the Indian sector of the Southern Ocean. Journal of Marine Systems, 17, 5-23.

Park, Y.-H., Charriaud, E., Riuz-Pino, D., Jeandel, C., 1998b. Seasonal and interranual variability of the mixed layer properties and steric height at station Kerfix, southwest of Kerguelen. Journal of Marine Systems, 17 (1-4), 575-586.

Park, Y.-H., Gamberoni, L., 1997. Cross-frontal exchange of Antarctic Intermediate Water and Antarctic Bottom Water in the Crozet Basin. Deep-Sea Research Part II, 44, 963-986.

Park, Y.-H., Gamberoni, L., 1995. Large-scale circulation and its variability in the South Indian Ocean from TOPEX/POSEIDON altimetry. Journal of Geophysical Research, 100, 24, 911-24,929.

Reyss, J.-L., Schmidt, S., Legeleux, F., Bonte, P., 1995. Large, low background well-type detectors for measurements of environmental radioactivity. Nuclear Instruments and Methods *A*, 357, 391-397.

Rutgers van der Loeff, M. M., Key, R.M., Scholten, J., Bauchs, D., Michel, A., 1995. 228Ra as a tracer for shelf water in the Arctic Ocean. Deep-Sea Research Part II, 42 (6), 1533-1553.

Rutgers van der Loeff, M. M., 1994. ^{228}Ra and ^{228}Th in the Weddell Sea. In : Johannessen , O.M., Muench, R.D., Overland, J.E. (Eds) : The Polar oceans and their role in shaping the global environment :The Nansen centennial volume. – Geophysical Monograph 85, 177-186, American Geophysical Union, Washington DC, USA.

Rutgers van der Loeff, M.M., Berger, G.W., 1993. Scavenging of ^{230}Th and ^{231}Pa near the Antarctic Polar Front in the South Atlantic. Deep-Sea Research Part I, 40, 339-357.

Sarmiento, J.L., Rooth, C.G.H., Broecker, W.S., 1982. Radium 228 as a tracer of basin wide processes in the abyssal ocean. Journal of Geophysical Research, 87, 9694-9698.

Sarmiento, J.L., Feely, H.W., Moore, W.S., Bainbridge, A.E., Broecker, W.S., 1976. The relationship between vertical eddy diffusion and buoyancy gradient in the deep sea. Earth and Planetary Science Letters, 32, 357-370.

Sarthou, G., Vincent, D., Christaki, U., Obernosterer, I., Timmermans, K.R., Brussaard, C.P.D., The fate of biogenic iron during a phytoplankton bloom induced by natural fertilization: impact of copepod grazing. Deep-Sea Research Part II, This issue.

Trull, T. W., and Armand, L., 2001. Insights into Southern Ocean carbon export from the $d^{13}C$ of particles and dissolved inorganic carbon during the SOIREE iron fertilisation experiment. Deep-Sea Research part II, 48(11/12), 2655-2680.

van Beek, P, François, R, Conte, M, Reyss, JL, Souhaut, M, Charette M, 2007. $^{226}Ra/^{228}Ra$ and $^{226}Ra/Ba$ ratios to track barite formation and transport in the water column. Geochimica Cosmochimica Acta, 71, 71-86.

Venchiarutti, C., Jeandel, C., Roy-Barman, M., Particle dynamics in the wake of Kerguelen Island traced by thorium isotopes (Southern Ocean, KEOPS program). submitted to Deep-Sea Research Part II.

Wagener, T., Guieu, C., Losno, R., Bonnet, S., Mahowald, N., Revisiting Atmospheric dust export to the South Hemisphere Ocean. submitted to Global biogeochemical cycles.

Zhang, Y., Lacan, F., Jeandel., C., Dissolved rare earth elements trace terrigeneous inputs in the wake of the Kerguelen Island (Southern Ocean). Deep-Sea Research Part II, This issue.

Figure caption

Figure 1 : Location of the stations investigated for ^{228}Ra and $^{228}Ra/^{226}Ra$ during KEOPS. The bathymetry of the Kerguelen Plateau is also shown.

Figure 2 : ^{228}Ra activities and $^{228}Ra/^{226}Ra$ ratios at stations Kerfix and C11, outside the Kerguelen Plateau. For information, ^{228}Ra concentration is also given in ag kg^{-1} (10^{-18} g kg^{-1}; *a* for *atto,* 10^{-18}). Open and solid squares represent ^{228}Ra activities and $^{228}Ra/^{226}Ra$ ratios obtained in nylon net samples. In the latter samples, the ^{228}Ra activities were obtained by combining the $^{228}Ra/^{226}Ra$ ratio measured in these samples with the ^{226}Ra activity of a sample collected with Niskin bottles at the same water depth. Arrows indicate samples below detection limit (see Table 1). Horizontal lines denote the depth of the bottom.

Figure 3 : ^{228}Ra activities and $^{228}Ra/^{226}Ra$ ratios at station A3 visited three times during KEOPS (A3-3, 23-24 Jan.; A3-4, 3-4 Feb.; A3-5, 12-13 Feb.), A3 being located on the Kerguelen Plateau in the middle of the phytoplankton bloom. Arrows indicate samples below detection limit (see Table 1). Horizontal lines denote the depth of the bottom.

Figure 4 : ^{228}Ra activities and $^{228}Ra/^{226}Ra$ ratios at stations C1, C5, B1 and B5 located on the Kerguelen Plateau. Arrows indicate samples below detection limit (see Table 1). Horizontal lines denote the depth of the bottom.

Figure 5 : Map showing the bathymetry in the area of the Kerguelen Plateau. This map allows us to locate sediments shallower than 200 m depth. The arrow on the Kerguelen Plateau indicates the circulation pattern of the upper ~150-m waters deduced from the ^{228}Ra activities in this study : waters that have interacted with the shallow lithogenic sediments surrounding

Heard Island are advected northward onto the Kerguelen Plateau (towards station A3). This pattern agrees with the northwestward flow of surface and subsurface waters reported by Charrassin et al.(2004) on the Kerguelen Plateau. The arrow south of Kerguelen Island indicates a strong current that is especially obvious from the plume of chlorophyll-poor waters (Blain et al., 2007).

Figure 6 : Estimate of the coefficient of vertical eddy diffusion (K_z) at station A3-3 using a simple one-dimensional diffusion model. K_z was estimated considering the decrease of the ^{228}Ra activities below the surface layer enriched in ^{228}Ra. The ^{228}Ra activity close to the bottom that likely reflects input from the sediment was excluded from the calculation. The line on the figure shows the best exponential fit considering ^{228}Ra data in the 100-400 m depth interval. Using equation (1), we calculate a K_z of $1.5.10^{-4} \pm 1.3.10^{-4}$ m^2 s^{-1}. The horizontal line denotes the depth of the bottom.

Table 1 : Dissolved ^{228}Ra activities and ^{228}Ra/^{226}Ra ratios measured during KEOPS at stations above and outside the Kerguelen Plateau.

The ^{228}Ra activities in nylon net samples were obtained by combining the ^{228}Ra/^{226}Ra ratio measured in these samples with the ^{226}Ra activity of a sample collected at the same water depth with Niskin bottles.

[1] : "UW" and "OISO" refer to samples collected using the ship seawater supply that provides seawater to the wet laboratory and to the ship seawater supply used for the continuous pCO_2 analysis, respectively (see Methods for details); "Pump" refers to samples collected using an *in situ* pump that returns water to the deck (0-120 m depth); "Nylon" refers to samples filtered using nylon nets (*in situ* deployment of 4 hours); The number of the CTD cast is reported for samples collected using Niskin bottles.

[2] : detection limit is based on twice the background noise; Arrows on the figures indicate activities below detection limit.

sc : short counting (< 17 h); only ^{226}Ra activities are reported; counting duration was too short to provide accurate ^{228}Ra activities. Samples with low counting statistics are reported in the Table only when counting duration was long (typically 3-5 days counting).

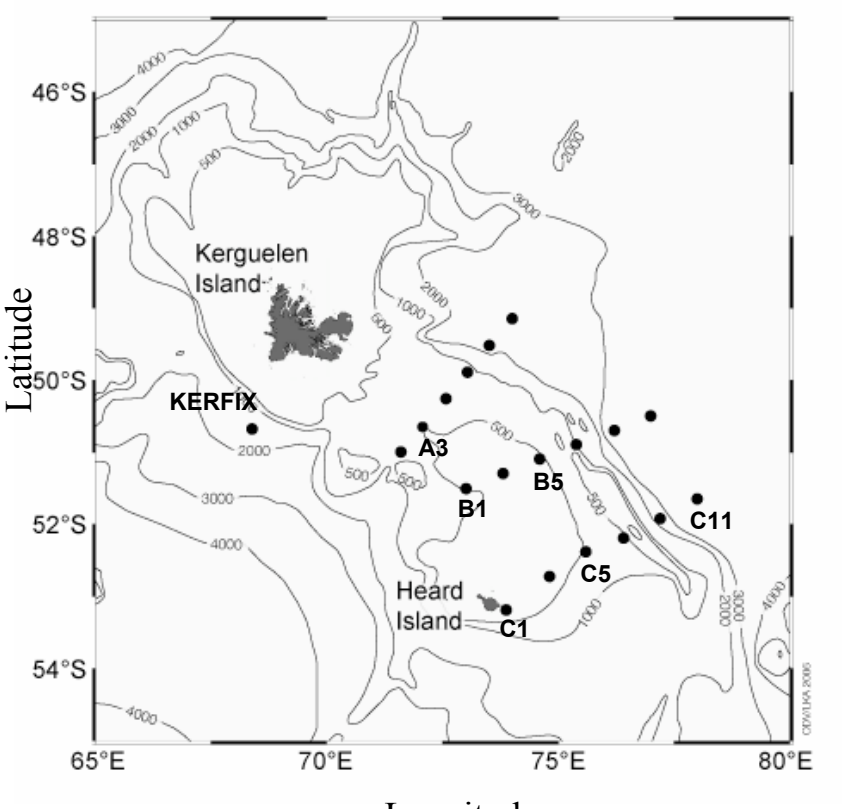
46°S
48°S
50°S
52°S
54°S
65°E
70°E
75°E
80°E
Latitude
Longitude
Kerguelen
Island
Heard
Island
KERFIX
A3
B1
B5
C1
C5
C11
4000
3000
2000
1000
500

Figure 1

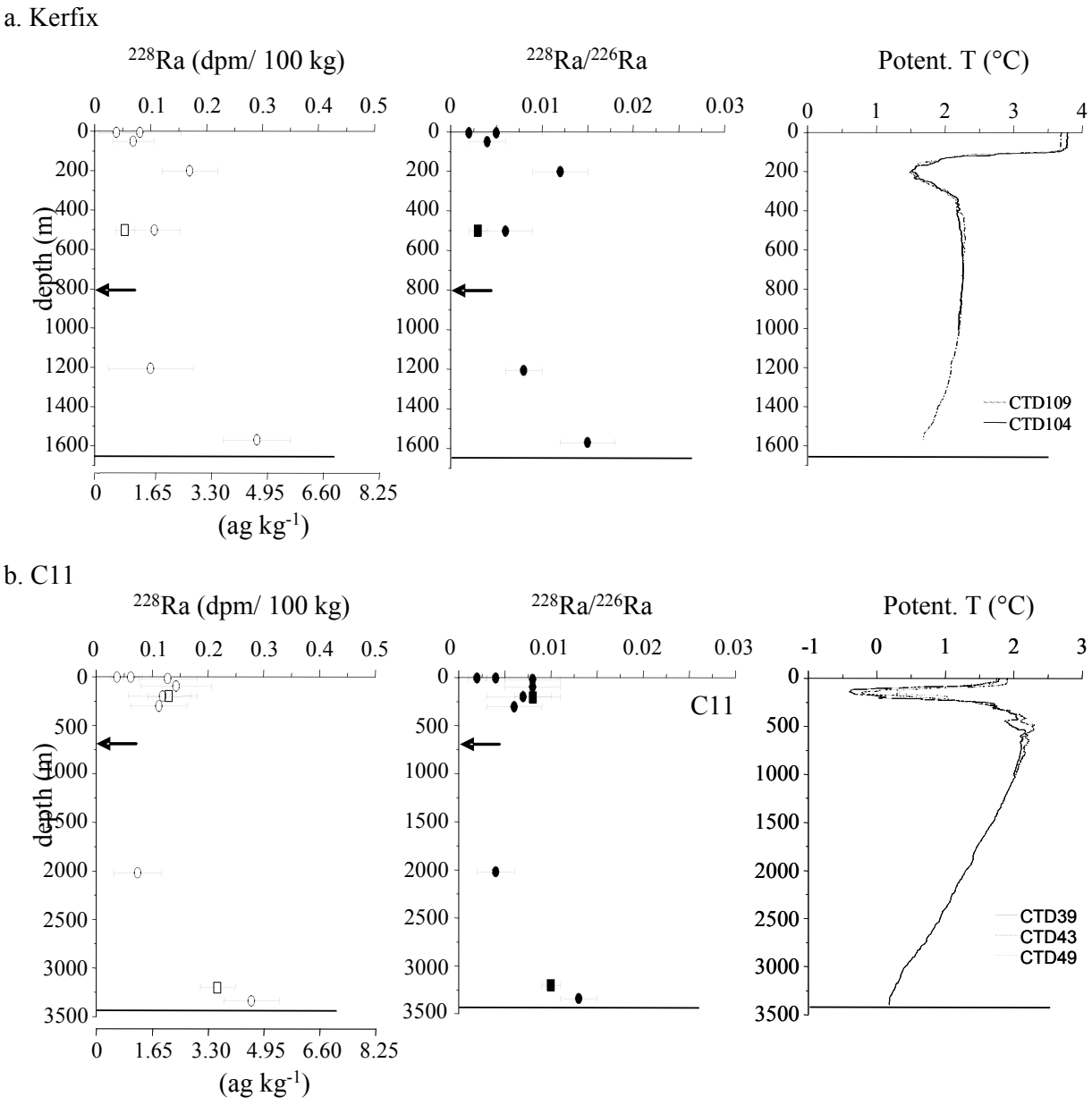
a. Kerfix
228Ra (dpm/ 100 kg)
228Ra/226Ra
Potent. T (°C)
depth (m)
(ag kg-1)
CTD109
CTD104
b. C11
228Ra (dpm/ 100 kg)
228Ra/226Ra
Potent. T (°C)
C11
depth (m)
(ag kg-1)
CTD39
CTD43
CTD49

Figure 2

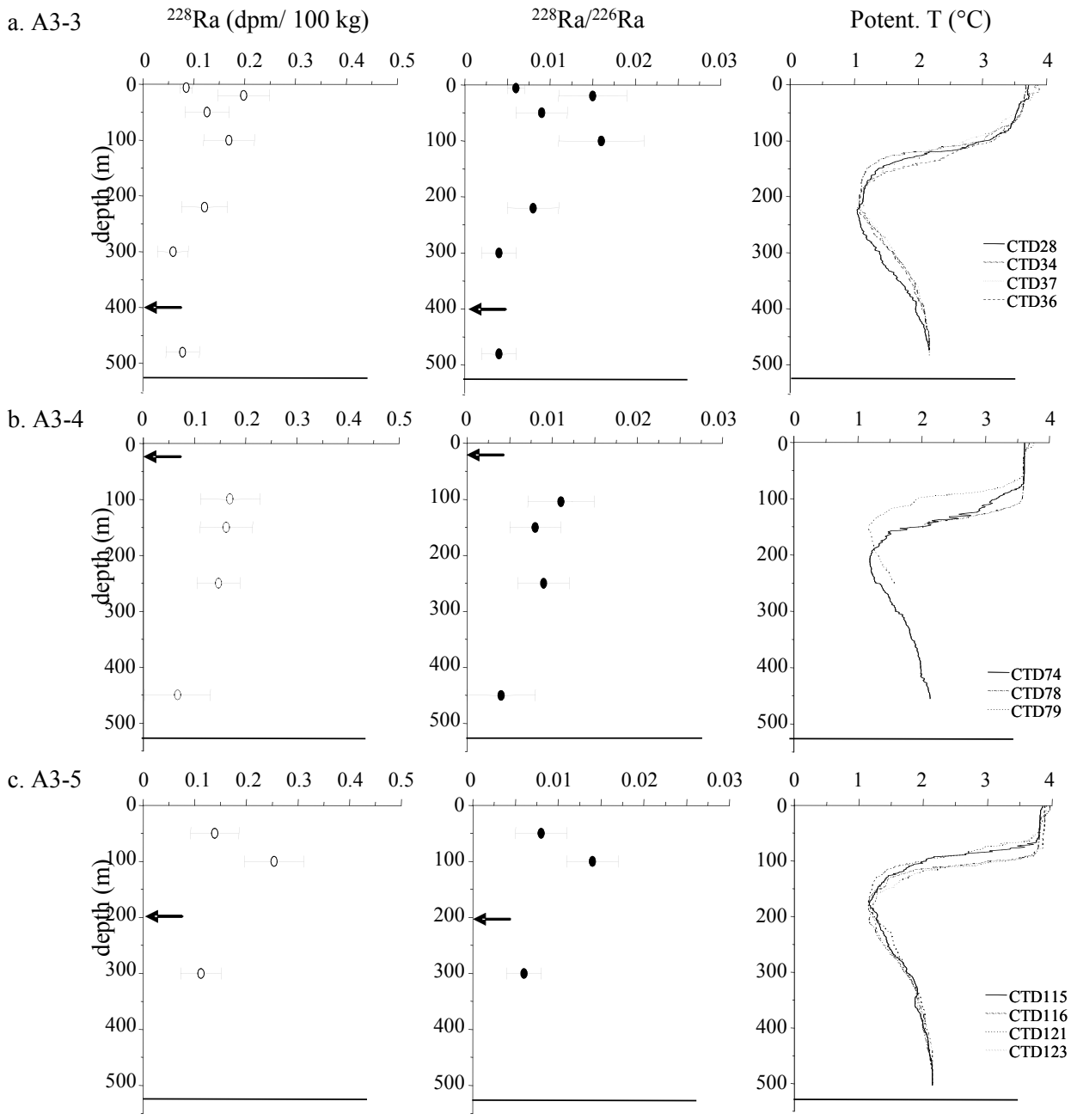
a. A3-3
^{228}Ra (dpm/ 100 kg)
^{228}Ra/^{226}Ra
Potent. T (°C)
depth (m)
CTD28
CTD34
CTD37
CTD36
b. A3-4
CTD74
CTD78
CTD79
c. A3-5
CTD115
CTD116
CTD121
CTD123

Figure 3

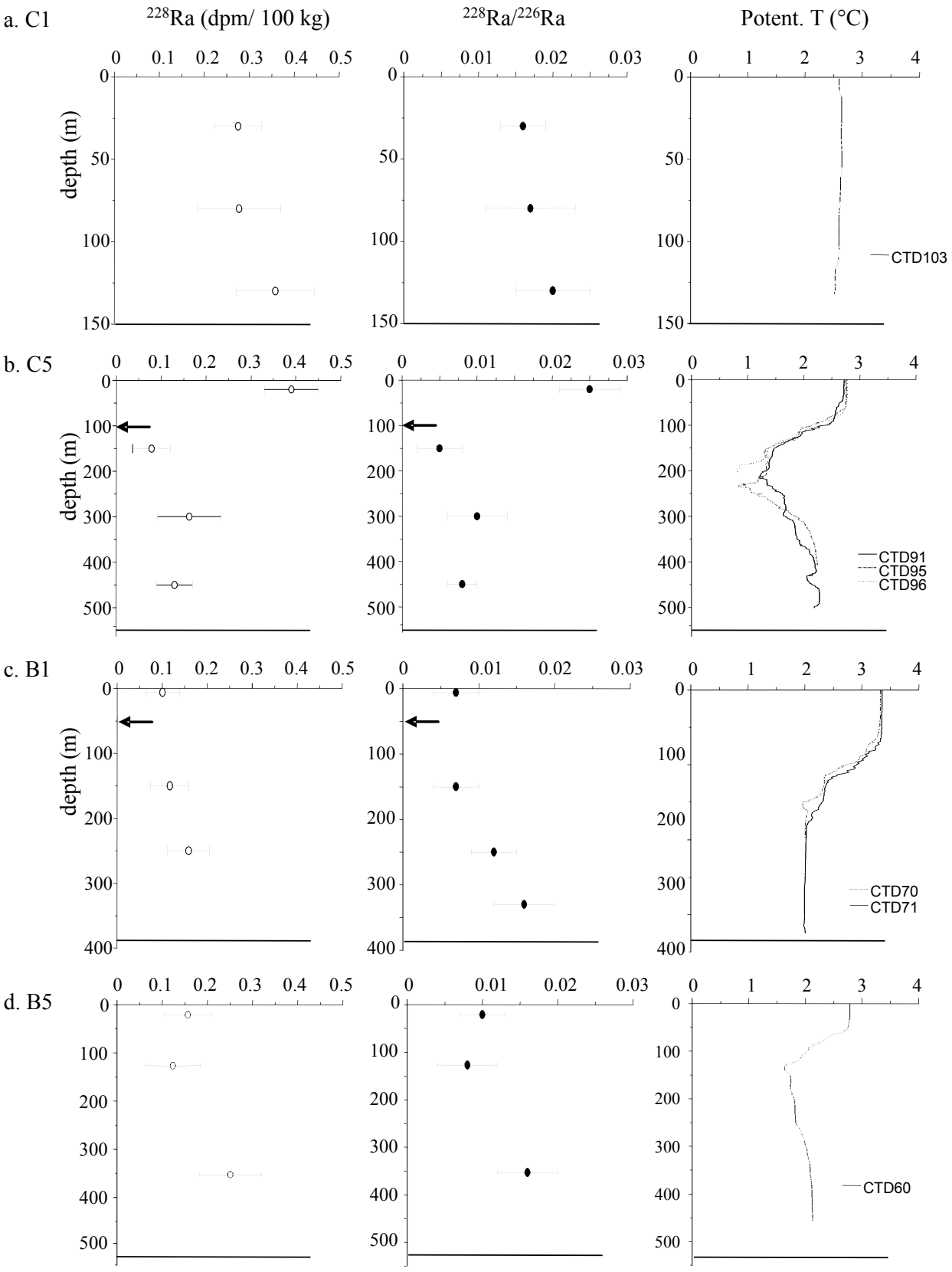
a. C1
^{228}Ra (dpm/ 100 kg)
^{228}Ra/^{226}Ra
Potent. T (°C)
depth (m)
CTD103
b. C5
depth (m)
CTD91
CTD95
CTD96
c. B1
depth (m)
CTD70
CTD71
d. B5
CTD60

Figure 4

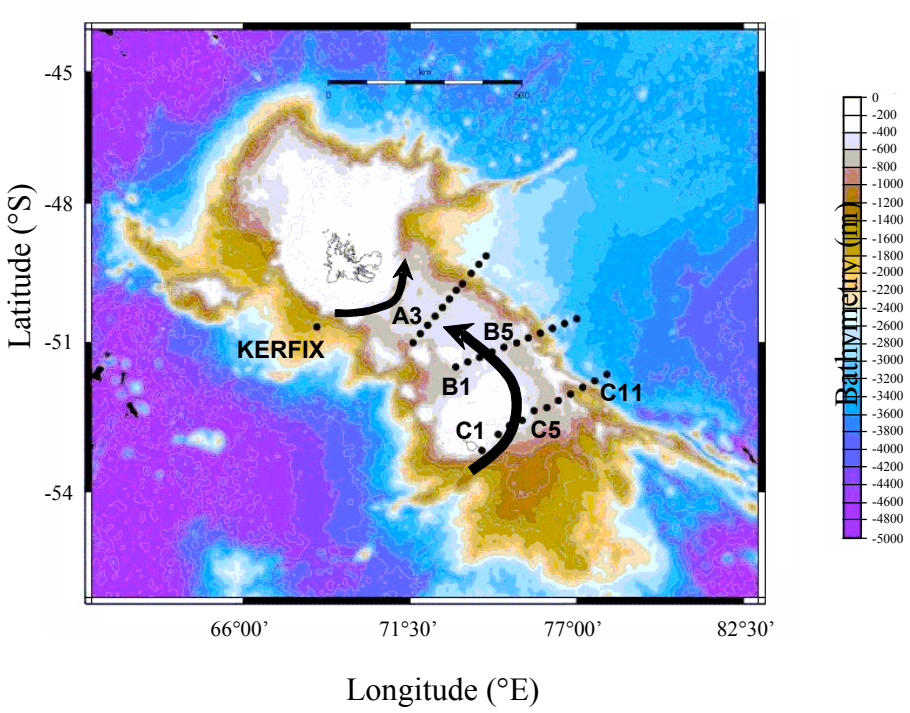
-45
-48
-51
-54
Latitude (°S)
66°00’
71°30’
77°00’
82°30’
Longitude (°E)
KERFIX
A3
B5
B1
C11
C1
C5
Bathymetry (m)
0
-200
-400
-600
-800
-1000
-1200
-1400
-1600
-1800
-2000
-2200
-2400
-2600
-2800
-3000
-3200
-3400
-3600
-3800
-4000
-4200
-4400
-4600
-4800
-5000

Figure 5

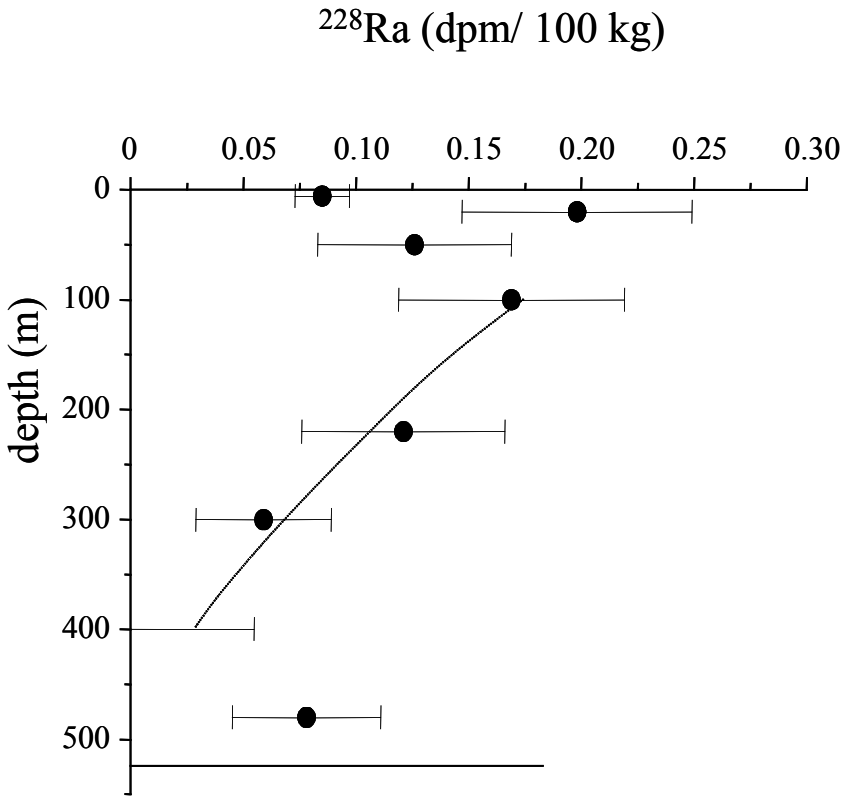
228Ra (dpm/ 100 kg)
0
0.05
0.10
0.15
0.20
0.25
0.30
depth (m)
0
100
200
300
400
500

Figure 6

Table 1

Depth	gamma	Sample[1]	Sampling date	Counting duration	Sample weight	^{226}Ra	^{226}Ra	^{228}Ra	^{228}Ra	^{228}Ra/^{226}Ra
m	theta			min	kg	dpm/ 100 kg	net counts	dpm/ 100 kg	net counts	
KERFIX										
6	26.88	UW	2/11/2005	970	557	15.9 ± 0.10	25681 ± 163	0.04 ± 0.040	29 ± 30	0.002 ± 0.003
6	26.88	OISO	2/11/2005	975	141	15.3 ± 0.19	6662 ± 84	0.08 ± 0.073	20 ± 18	0.005 ± 0.005
51	26.87	CTD #104	2/10/2005	4366	85	16.2 ± 0.12	19160 ± 142	0.07 ± 0.037	57 ± 30	0.004 ± 0.002
202	27.16	CTD #104	2/10/2005	5941	99	14.6 ± 0.11	27176 ± 171	0.17 ± 0.050	138 ± 51	0.012 ± 0.003
500	27.45	Nylon	2/10/2005	5590			111191 ± 340	0.06 ± 0.019	187 ± 63	0.003 ± 0.001
502	27.45	CTD #104	2/10/2005	3921	97	17.3 ± 0.12	20764 ± 148	0.11 ± 0.046	75 ± 32	0.006 ± 0.003
806	27.61	CTD #109	2/11/2005	4552	102	16.9 ± 0.11	24804 ± 161	<0.07 [2]		
1207	27.73	CTD #109	2/11/2005	5665	96	18.7 ± 0.11	32193 ± 183	0.10 ± 0.076	25 ± 19	0.008 ± 0.002
1571	27.80	CTD #109	2/11/2005	4147	99	19.3 ± 0.13	25050 ± 162	0.29 ± 0.060	88 ± 35	0.015 ± 0.003
C11										
6	27.04	UW	1/25/2005	2538	3005	14.9 ± 0.03	340766 ± 594	0.04 ± 0.011	351 ± 102	0.002 ± 0.001
6	27.04	OISO	1/26/2005	7954	274	17.1 ± 0.05	117679 ± 350	0.06 ± 0.020	203 ± 66	0.004 ± 0.001
21	27.05	Pump	1/26/2005	4216	104	16.1 ± 0.11	22316 ± 153	0.13 ± 0.052	85 ± 35	0.008 ± 0.003
99	27.18	Pump	1/26/2005	2883	103	18.0 ± 0.14	16940 ± 134	0.14 ± 0.063	66 ± 29	0.008 ± 0.003
150	27.29	CTD #49	1/28/2005	248	138	17.3 ± 0.45	1608 ± 41	sc		
201	27.34	CTD #49	1/28/2005	4268	68	16.9 ± 0.14	15637 ± 130	0.12 ± 0.062	64 ± 33	0.007 ± 0.004
200	27.36	Nylon	1/25/2005	5722			38444 ± 201	0.13 ± 0.059	143 ± 42	0.008 ± 0.003
303	27.48	CTD #43	1/28/2005	4216	95	18.2 ± 0.12	23205 ± 156	0.11 ± 0.050	73 ± 33	0.006 ± 0.003
706	27.67	CTD #43	1/28/2005	4040	96	18.2 ± 0.13	22362 ± 154	<0.08 [2]		
1010	27.74	CTD #43	1/28/2005	186	94	17.6 ± 0.63	841 ± 30	sc		
2021	27.81	CTD #39	1/25/2005	5656	132	19.9 ± 0.10	20708 ± 147	0.07 ± 0.042	82 ± 47	0.004 ± 0.002
3200	27.85	Nylon	1/25/2005	5630			102590 ± 326	0.22 ± 0.031	436 ± 63	0.010 ± 0.001
3343	27.83	CTD #39	1/25/2005	4431	138	22.2 ± 0.11	43020 ± 212	0.28 ± 0.049	240 ± 42	0.013 ± 0.002
A3-3										
6	26.94	UW	1/24/2005	5586	949	14.1 ± 0.03	223327 ± 481	0.09 ± 0.013	592 ± 87	0.006 ± 0.001
20	26.94	CTD #28	1/23/2005	5579	140	13.4 ± 0.08	28304 ± 175	0.20 ± 0.051	182 ± 47	0.015 ± 0.004
51	26.95	CTD #34	1/24/2005	7085	128	13.4 ± 0.08	32958 ± 188	0.13 ± 0.043	142 ± 49	0.009 ± 0.003
102	27.02	CTD #34	1/24/2005	3579	139	10.4 ± 0.08	16405 ± 133	0.17 ± 0.051	122 ± 38	0.016 ± 0.005
223	27.24	CTD #36	1/24/2005	5195	136	15.4 ± 0.09	34458 ± 191	0.12 ± 0.045	127 ± 47	0.008 ± 0.003
304	27.32	CTD #36	1/24/2005	7085	132	16.3 ± 0.08	48365 ± 227	0.06 ± 0.030	107 ± 53	0.004 ± 0.002
404	27.43	CTD #37	1/24/2005	5664	133	14.8 ± 0.09	30325 ± 180	<0.054 [2]		
484	27.47	CTD #37	1/24/2005	5664	141	17.5 ± 0.09	44091 ± 215	0.08 ± 0.033	109 ± 46	0.004 ± 0.002
A3-4										
19.9	26.95	Pump	2/4/2005	4201	137	14.1 ± 0.09	25535 ± 163	<0.053 [2]		
98.3	27.04	Pump	2/4/2005	4201	138	15.6 ± 0.11	24442 ± 161	0.17 ± 0.059	106 ± 37	0.011 ± 0.004
151	27.12	CTD #78	2/4/2005	4305	105	20.1 ± 0.13	25642 ± 164	0.16 ± 0.051	102 ± 32	0.008 ± 0.003
253	27.31	CTD #79	2/4/2005	5647	102	15.9 ± 0.10	28939 ± 174	0.15 ± 0.042	129 ± 37	0.009 ± 0.003
455	27.45	CTD #74	2/3/2005	4293	85	16.5 ± 0.13	16352 ± 132	0.07 ± 0.064	33 ± 31	0.004 ± 0.004
A3-5										
50	26.93	CTD #115	2/12/2005	4170	139	16.7 ± 0.10	27130 ± 169	0.14 ± 0.047	110 ± 37	0.008 ± 0.003
100	26.99	CTD #116	2/12/2005	2794	139	18.2 ± 0.12	22398 ± 153	0.25 ± 0.057	148 ± 33	0.014 ± 0.003
201	27.26	CTD #121	2/12/2005	4224	141	16.3 ± 0.10	26332 ± 166	<0.051 [2]		
301	27.33	CTD #123	2/13/2005	4619	139	17.5 ± 0.09	35573 ± 193	0.11 ± 0.039	110 ± 38	0.006 ± 0.002
B1										
6	26.97	OISO	2/2/2005	5722	143	14.8 ± 0.08	32980 ± 186	0.10 ± 0.037	110 ± 40	0.007 ± 0.003
50	26.97	CTD #70	2/2/2005	5678	87	14.5 ± 0.11	19475 ± 144	<0.08 [2]		
150	27.15	CTD #70	2/2/2005	5678	97	16.4 ± 0.10	28501 ± 173	0.12 ± 0.043	106 ± 39	0.007 ± 0.003
251	27.23	CTD #71	2/2/2005	4310	131	13.6 ± 0.09	24429 ± 161	0.16 ± 0.047	130 ± 38	0.012 ± 0.003
324	27.29	CTD #71	2/2/2005	5722	133		16013 ± 131		123 ± 32	0.016 ± 0.004
B5										
21	27.03	Pump	2/1/2005	4190	137	16.3 ± 0.10	29448 ± 176	0.16 ± 0.052	119 ± 39	0.010 ± 0.003
127	27.16	Pump	1/31/2005	4205	137	15.2 ± 0.10	25063 ± 163	0.12 ± 0.058	74 ± 35	0.008 ± 0.004
353	27.43	CTD #60	2/1/2005	4224	99	15.8 ± 0.11	20806 ± 149	0.25 ± 0.069	136 ± 38	0.016 ± 0.004
C1										
30	27.06	Pump	2/9/2005	4232	97	16.8 ± 0.12	21862 ± 151	0.28 ± 0.053	174 ± 34	0.016 ± 0.003
81	27.07	CTD #103	2/9/2005	2825	95	16.3 ± 0.14	14252 ± 124	0.28 ± 0.093	108 ± 36	0.017 ± 0.006
132	27.09	CTD #103	2/9/2005	2899	84	17.6 ± 0.16	13593 ± 120	0.36 ± 0.087	121 ± 29	0.020 ± 0.005
C5										
20	27.02	Pump	2/8/2005	5197	138	15.6 ± 0.09	30299 ± 180	0.39 ± 0.063	304 ± 49	0.025 ± 0.004
100	27.05	Pump	2/8/2005	5795	141	15.4 ± 0.09	34173 ± 192	<0.051 [2]		
151	27.18	CTD #96	2/8/2005	7025	97	16.4 ± 0.09	35282 ± 195	0.08 ± 0.043	99 ± 53	0.005 ± 0.003
202	27.25	CTD #95	2/8/2005	951	94	14.4 ± 0.25	3513 ± 61	sc		
301	27.35	CTD #95	2/8/2005	7025	97	16.7 ± 0.10	30895 ± 184	0.16 ± 0.071	122 ± 53	0.010 ± 0.004
405	27.44	CTD #95	2/8/2005	976	97	16.5 ± 0.24	4949 ± 72	sc		
453	27.47	CTD #91	2/7/2005	5620	119	16.3 ± 0.09	34509 ± 191	0.13 ± 0.040	130 ± 42	0.008 ± 0.002